PAPER

Check for updates

The modulation of tumor-associated macrophages *via* natural nanomodulators by neutralizing the acidic tumor microenvironment for tumor treatment†

Lei Peng,[a] Chenxu Zhang,[a] Guanlun Zhou,[a] Ao Yu*[bc] and Yongjian Wang ✆ *[a]

Tumor-associated macrophages (TAMs) account for nearly half the mass of solid tumors. A number of studies show that TAMs are similar to M2 macrophages, which have strong immunosuppressive activity. Manipulation of the phenotype of TAMs is a novel and potential therapeutic approach to enhance antitumor immunity. Based on this, this paper comprehensively reveals that immunomodulator β-glucan (Glu) could not fully exert its role in reversing macrophage polarization under acidic conditions, and calcium carbonate improved the role of Glu by neutralizing the acidic environment. To be specific, by constructing a Glu and calcium carbonate co-precipitation system (Glu-VCC), Glu-VCC could exhibit a stronger immune-activating effect through a cascade reaction with its ability to continuously regulate the tumor microenvironment. Glu-VCC nanoparticles can raise the pH of the tumor tissue from 6.7 to 7.0 and increase M1-like macrophages by 57% compared to the limited reversal ability of Glu toward TAMs. In addition, Glu-VCC showed excellent tumor clearance in *in vivo* experiments. These results not only expand the use of calcium carbonate in the delivery of drugs but also provide new ideas for tumor immunotherapy.

Introduction

Macrophages are very important immune cell types in the human body, most of which are derived from bone marrow monocytes.[1] Under the influence of different microenvironmental signals, macrophages polarize into two functional phenotypes, namely classically-activated macrophages (M1) and alternatively-activated macrophages (M2).[2] In contrast to the pro-inflammatory as well as tumoricidal effects of M1, M2 has anti-inflammatory and tumorigenic effects.[3,4] Despite the complexity of macrophage phenotypes in the tumor microenvironment, it is evident that tumor-associated macrophages (TAMs) more closely resemble M2 macrophages. As a type of cell possessing adjustable polarity, M2-like TAMs can be re-educated to a tumor-killing M1 type,[5–7] providing an attractive target for cancer immunotherapy.[8–13] To promote the

transformation of TAMs into M1 macrophages, several reagents, such as monoclonal antibodies, kinase inhibitors, and cytokines, were applied to repolarize TAMs.[14–16] Yeast-derived β-glucan (Glu), a polysaccharide, is a potent immunomodulator that is shown to possess anticancer properties[17] and is proven to have the ability to reverse M2-like TAMs into M1-like TAMs.[18] However, it was found that Glu treatment has no significant effect on M2-like macrophage-related factor IL-10, which probably restricts the final antitumor effect.[19] It is worth mentioning that the expression of IL-10 in macrophages is significantly enhanced in tumor acidic microenvironments, and the expression and secretion of IL-10 is an important marker of TAM polarization to M2-like TAMs.[11,20,21]

The formation of a weak acidic microenvironment in solid tumors is inextricably linked to the presence of lactic acid (LA).[22–25] Compared to normal cells, the growth of cancer cells is heavily dependent on glycolysis, a process that produces a large amount of LA.[26] There is growing evidence that LA in the tumor microenvironment can exert immunosuppressive effects by inducing and recruiting immunosuppression-related cells and molecules, thereby promoting tumor progression.[27,28] Some researchers pointed out that LA plays a central role in the polarization of TAMs to M2 macrophages.[29] Toszka Bohn's research directly indicated that the acidification of tumors contributed to the functional polarization of TAMs and

[a] *Key Laboratory of Bioactive Materials, Ministry of Education, College of Life Sciences, Nankai University, Tianjin 300071, China.*
E-mail: yongjian_wang@nankai.edu.cn
[b] *Haihe Laboratory of Sustainable Chemical Transformations, Tianjin 300192, China*
[c] *Tianjin Key Laboratory of Molecular Recognition and Biosensing, College of Chemistry, Nankai University, Tianjin, 300071, China. E-mail: esr@nankai.edu.cn*
† Electronic supplementary information (ESI) available. See DOI: https://doi.org/10.1039/d3ma00243h

promoted tumor growth.[30] The researchers also found that TAMs expressed a variety of pH-sensitive G protein-coupled receptors and thus could adjust their behavior according to changes in the extracellular pH (pHe).[31] In conclusion, improving or reversing the acidic microenvironment caused by LA in tumors may affect TAM phenotypes.[9]

There are various options to modify the acidic microenvironment of tumors. Tumor-derived lactate is an attractive tumor immunotherapy target. Exhausting lactate by lactate oxidase in tumor cells and TME shows a good effect on immunotherapy.[32,33] Decreased extracellular lactate content to regulate the TME can also be achieved by inhibiting the efflux of intracellular lactate by silencing the expression of MCT-4 (monocarboxylate transporter-4) with MCT4-inhibiting siRNA.[34] Besides, it is an easy way to modify the acidic TME by sodium bicarbonate. Tumor cells could be killed under glucose starvation or deficiency quickly and effectively using sodium bicarbonate to remove hydrogen ions from the tumor. Because water-soluble sodium bicarbonate $in\ situ$ can only be injected, it is difficult to meet the treatment of deep lesions. In addition, excessive sodium bicarbonate may cause alkalosis in humans.[35] As a novel drug delivery vehicle, calcium carbonate ($CaCO_3$) is particularly prominent for its direct modulation of the acidic microenvironment in the tumor area as well as its high drug loading and excellent biocompatibility.[36–40] The most important aspect is that $CaCO_3$ does not decompose in the environment above pH 7.4, thus avoiding the defects of alkali poisoning seen with other reagents.[41–43] To date, there are fewer studies on the influence of TAM polarization through $CaCO_3$-regulated pH in the tumor environment, in particular, whether $in\ vivo$ $CaCO_3$ can elicit the same immune response. The elucidation of these questions is crucial for future applications of $CaCO_3$ NPs in the field of oncology.

In this study, we constructed a macrophage polarization model using LA to simulate the acidic microenvironment of tumors $in\ vivo$. Natural nanomodulators (Glu-VCC) were obtained by the co-precipitation of Glu with calcium carbonate. $CaCO_3$ acts as a tumor-acidic environment pH-sensitive responsive nanocarrier to load Glu as a potential strategy to enhance the immunomodulatory capacity of Glu (Scheme 1). By immunofluorescence staining of CD206 (M2 related) and CD86 (M1 related) markers on the surface of the macrophages,[44,45] as well as the quantitative analysis of two cytokines IL-10 (M2 related) and IL-12 (M1 related), the inhibition ability of Glu-VCC on the differentiation of macrophages into the M2 type induced by LA was verified in RAW264.7 cells. Besides, the changes in the microenvironment pH of the solid tumors induced by Glu-VCC were monitored by probe detection. The $in\ vivo$ remodeling effect on TAMs and tumor inhibition ability of Glu-VCC were evaluated in 4T1 tumor-bearing Babl/c mice. In conclusion, this paper reveals the inhibitory effect of the tumor acidic microenvironment on the role of β-glucan in reversing macrophage polarization and the relieving effect of calcium carbonate on the inhibition effect. More importantly, we hope to advance the application of calcium carbonate nanoparticles in tumor immunotherapy.

Results and discussion

Characterization of Glu-VCC nanoparticles

In this study, Glu-VCC nanoparticles were constructed by encapsulating Glu in calcium carbonate by coprecipitation. Glu-VCC was observed to be of regular spherical shape and uniformly dispersed (Fig. 1a and b). Elemental analysis showed that Ca and O elements were uniformly distributed throughout the nanoparticles (Fig. 1c), and the average hydrated particle size was 105 nm (Fig. 1d). Zeta potential of Glu-VCC was −19.4 mV, which was determined by DLS (Fig. S1, ESI†). The successful preparation of Glu-VCC was also verified by Fourier infrared spectroscopy, a C–H stretching vibration peak at 2800 cm^{-1}, an O–H stretching vibration peak at 3300 cm^{-1}, and C–O stretching vibrations at 1100 cm^{-1} were found compared with $CaCO_3$ (Fig. 1e). The mass ratios of β-glucan and $CaCO_3$ in GLU-VCC was 1 : 9, which was determined by the Congo Red test. The XRD results showed that the $CaCO_3$ in Glu-VCC was vaterite calcium carbonate, as shown in Fig. 1f. Glu-VCC is stable in PBS and cell culture DMEM containing 10% fetal bovine serum, and discomposes in a weakly acidic buffer (Fig. S2, ESI†). These results suggested that Glu-VCC has tumor-targeting capability. Calcium carbonate nanoparticles
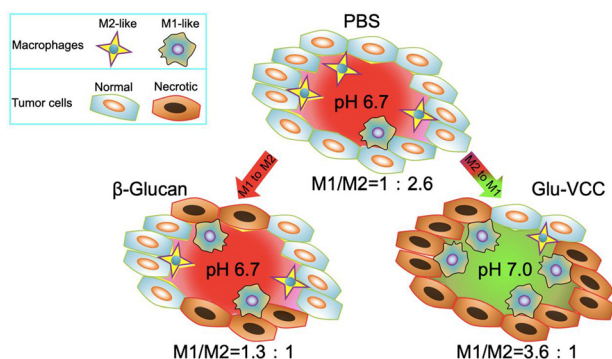
Scheme 1 Glu-VCC increases the extracellular pH of the solid tumor from 6.7 to 7.0, thus significantly repolarizing TAMs to the M1 subtype.
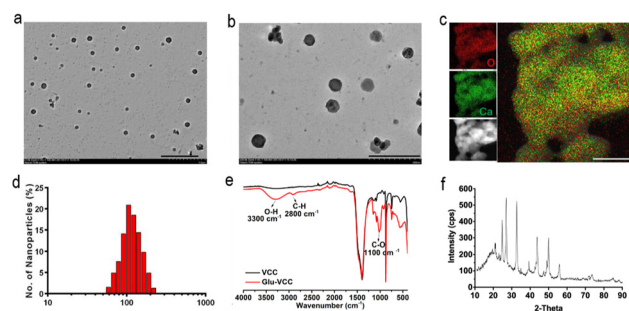

Fig. 1 The characterization of Glu-VCC nanoparticles: (a) transmission electron microscopy, scale bar: 1 μm; (b) amplified transmission electron microscopy, scale bar: 500 nm; (c) X-ray energy spectrometry analysis of Glu-VCC nanoparticles and the Ca and O elements, scale bar: 50 nm; (d) the particle size distribution of Glu-VCC nanoparticles; (e) the Fourier infrared spectra of Glu-VCC and VCC nanoparticles and (f) the XRD pattern of Glu-VCC.

(VCC) were used as a control and characterized, as shown in Fig. S3 (ESI†). Glucan used in this study was water soluble.

Glu-VCC continuously regulates the tumor's acidic microenvironment both *in vitro* and *in vivo*

The acidic microenvironment is known to be a characteristic feature of tumors. This is because glycolysis in cancer cells produces not only ATP but also large amounts of LA.[46] We first accurately quantified the LA contents and the pH of the culture media after cells were incubated for 4 days. In the medium of the lung cancer cells (LLC), the LA content was as high as 38 mM, and the pH value was 6.5. In the media of hepatoma cells (H22) and breast cancer cells (4T1), the LA contents were approximately 25 mM, and the pH was approximately 6.7. In the medium of LO2 cells, normal human hepatocytes, the LA content was as low as 10 mM and the pH was nearly 7.0 (Fig. 2a and b). These indicated that tumor cells produced more LA than normal cells during *in vitro* incubation. Although the amount of LA was varied for different cell lines, it was positively associated with the acidity in the culture medium.
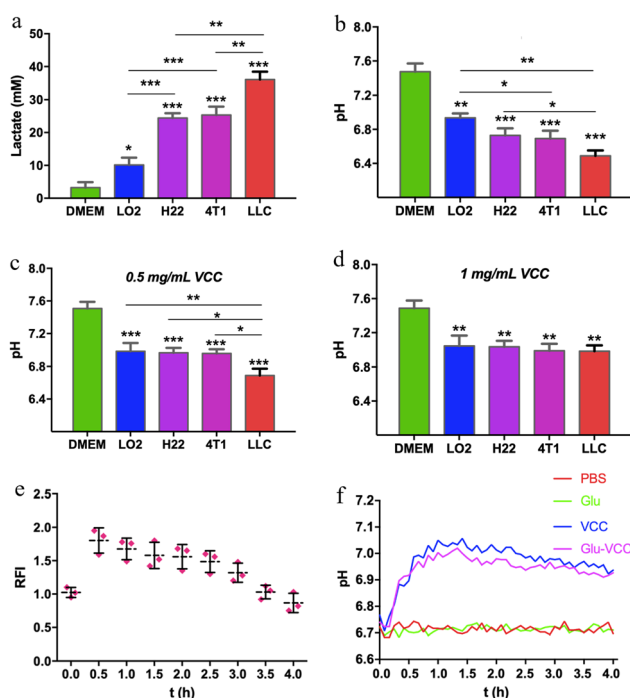

Fig. 2 The modulation of pH by VCC and Glu-VCC nanoparticles *in vitro* and *in vivo*. (a) The LA content in the culture medium and media incubated with cells; (b) the pH of the culture medium and media incubated with cells; (c) the pH of VCC nanoparticle-containing culture media and VCC nanoparticle-containing media incubated with cells (VCC = 0.5 mg mL^{-1}); (d) the pH of VCC nanoparticle-containing culture media and VCC nanoparticle-containing media incubated with cells (VCC = 1 mg mL^{-1}). The incubation time was 4 days; (e) relative fluorescence intensity of the red sector region in ICR mice at each time point and (f) the pHe curve in PBS, Glu, VCC, and Glu-VCC treatment groups within 4 hours in the tumor of Balb/c mice. The data were collected every 5 minutes. The * above the bar graph was compared with the cell-free medium group, n = 3, and * represents $p < 0.05$, ** stands for $0.0001 < p < 0.05$, *** stands for $p < 0.0001$.

Researchers have demonstrated that specific sizes of calcium carbonate nanoparticles can modulate the acidic environment of cancer.[42] To validate the pH-regulating ability of the calcium carbonate nanoparticles we prepared, VCC was added to the medium (final concentration was 0.5 mg mL^{-1}) and incubated with the cells for 4 days. The pH of the LO2 cell culture medium remained at 7.0 without any obvious change. The pH of 4T1 and H22 cell culture media was 6.9, and that of the LLC medium was 6.7. When the concentration of VCC increased to 1 mg mL^{-1}, the pH values of all the culture media were about 7.0, as shown in Fig. 2c and d. This indicated that VCC effectively scavenged H$^+$, without alkalizing the pH of the culture media. Therefore, calcium carbonate provides an excellent margin of safety for reversing an acidic microenvironment.

To further prove the effect of Glu-VCC on *in vivo* modulating of the acidity of the tumor, BCECF (a pH-sensitive probe, whose fluorescence intensity is positively correlated with pH) was used to monitor the pHe of the tumor. For better observations, H22 xenografts were implanted under the abdominal cortex of ICR mice (shown in the red sector of Fig. S4, ESI†). After subcutaneous injection of 100 μL of 1 mM BCECF, 200 μL of 20 mg mL^{-1} Glu-VCC nanoparticles were subsequently injected into the mouse through the tail vein. Images were collected every half hour using an animal living imaging system, and yellowish spots with higher fluorescence intensity appeared in the tumor area at 0.5 h and steadily decreased over time. The fluorescence intensity at 0.5 h was approximately 1.8 times that at 0 h, which proved that Glu-VCC could increase the pHe, as shown in Fig. 2e.

To improve the accuracy and effective detection of pH measurement, a micro pH composite electrode (LabSen 242-3, diameter 3 mm) was inserted into the tumor of a 4T1 tumor-bearing Balb/c mouse for continuous pH monitoring. As shown in Fig. 2f, the pHe of the tumor was around 6.7. After an intravenous injection of 200 μL 20 mg mL^{-1} Glu-VCC, the pHe increased significantly. After 30 minutes of the injection, the pHe of Glu-VCC-treatment increased to 6.9. After 60 minutes, the pHe reached 7.0 and remained stable for the next 30 minutes without any further increase. The pHe began to decline gradually after 90 minutes, but the decline rate was slow. The pHe remained at 6.9 for 240 minutes. However, PBS or Glu did not affect the pHe. These results suggested that Glu-VCC nanoparticles were an effective H$^+$ scavenger that could upregulate pHe to approximately 7.0, without further excessive elevation, avoiding the risk of alkaloid toxicity.

Glu-VCC reprogram LA-induced RAW264.7 cells *in vitro*

The culture medium containing 25 mM LA was used to stimulate undifferentiated RAW264.7 cells. The results showed that the M2-like macrophage marker CD206 was abundantly produced on the cell surface, while there was little signal of M1-like marker CD86 (Fig. 3a). As a control group, under the stimulation of the classical stimulant lipopolysaccharide (LPS), a large amount of CD86 and a small CD206 signal appeared on the surface of the RAW264.7 cells (Fig. 3b), indicating that the cells successfully differentiated into M1 under LPS stimulation.
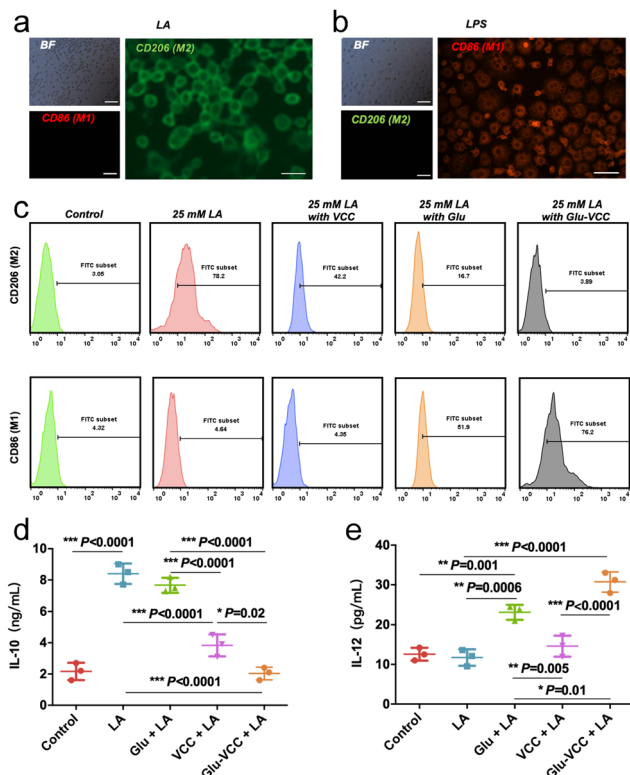
Fig. 3 Glu-VCC reprogram for LA-induced RAW264.7 cells *in vitro*. RAW264.7 staining with M2-like macrophage markers CD206 and M1-like macrophage CD86 after stimulation with (a) LA, scale bar = 50 μm and (b) LPS, scale bar = 50 μm; BF stands for bright field observation. (c) Flow cytometry analysis of the expression of CD206 and CD86 on the surface of RAW264.7 cells in the control group (PBS), LA, LA + VCC, LA + Glu, and LA + Glu-VCC. (d) IL-10 secretion and (e) IL-12 secretion in the medium, $n = 3$. The * above the bar graph was compared with the cell-free medium group, $n = 3$, and * represents $p < 0.05$, ** stands for $0.0001 < p < 0.05$, *** stands for $p < 0.0001$.

This confirms that LA induces polarization of RAW264.7 cells to the M2 type.

Flow cytometry was used to detect the phenotype of TMAs after various treatments (Fig. 3c). When VCC was added to the LA-containing culture medium, CD206^{hi} RAW264.7 cells decreased from 78.2% to 42.2%, but CD86^{hi} RAW264.7 showed no significant change. The result indicated that VCC inhibited the differentiation of LA-induced macrophages to the M2 phenotype but did not reverse the macrophages to the M1 phenotype. However, after adding 200 μg of Glu to LA-containing DMEM, CD86^{hi} RAW264.7 cells accounted for only 51.9%, and there was still 16.7% of CD206^{hi} RAW264.7 cells. After adding Glu-VCC to the LA-containing medium, CD86^{hi} RAW264.7 increased to 76.2%, while only 3.89% of CD206^{hi} RAW264.7 remained. According to the above results, Glu could not convert all RAW264.7 cells to M1-like cells. It is noteworthy that CD86^{hi} RAW264.7 increased to 76.2% and CD206^{hi} RAW264 was only 3.89% in the presence of Glu-VCC.

Macrophages with different phenotypes exercise their pro-inflammatory or anti-inflammatory functions relying on their secreted interleukin. Previous studies have shown that the acidic environment induces macrophage secretion of IL-10 (cytokine secreted by the M2-like phenotype) in large amounts, and the expression of IL-10 in the tumor area decreased after removing H$^+$ from the tumor area.[11,20] These results indicate that the expression and secretion of IL-10 are positively corre-lated with the tumor acid microenvironment. Therefore, we speculated that improving the pH of the acidic microenviron-ment in the tumor tissues by VCC can inhibit the secretion of IL-10 and improve the anti-tumor efficacy of Glu. To test this hypothesis, the secreted IL-10 in the media was detected using an ELISA kit when RAW264.7 cells were treated with VCC, Glu, and Glu-VCC in the LA-containing media (Fig. 3d). In the control group (the medium without LA), the secretion of IL-10 was only 2.17 ng mL^{-1}, but the IL-10 secretion increased rapidly to 8.40 ng mL^{-1} after LA was added to the medium. Glu could not effectively change the level of IL-10 (7.67 ng mL^{-1}) induced by LA. VCC nanoparticles rapidly inhibited the secretion of IL-10 (3.83 ng mL^{-1}), possibly due to the elimination of H$^+$ in the medium. Notably, the secretion of IL-10 (2.03 ng mL^{-1}) in the Glu-VCC group was lower than that in the VCC group. This result indicated that Glu-VCC can continuously reduce M2-like macrophages, which are important sources of IL-10 secretion, thus leading to a further reduction of IL-10 in the medium.

In addition, we also detected the M1-like macrophage secre-tory marker IL-12, as shown in Fig. 3e. The secretion of IL-12 did not change significantly before and after LA stimulation, and the expressions were approximately 12 pg mL^{-1}, suggesting that LA could not affect the secretion of IL-12. In the VCC group, the secretion level of IL-12 was 14.60 pg mL^{-1}, which was not significantly different from that in the LA-containing medium without VCC. It was further demonstrated that the depletion of H$^+$ from the medium did not affect the secretion of IL-12, which was consistent with the inability of VCC to increase the expression of the M1-like macrophage marker CD86. However, Glu significantly increased the expression of IL-12 in RAW264.7 cells to 23.13 pg mL^{-1}, which was higher than that in the LA-containing medium without Glu. In the Glu-VCC group, the secretion of IL-12 increased to 30.73 pg mL^{-1}. These suggest that calcium carbonate and Glu have different effects on the polarization of RAW264.7 cells and the secretion of interleukin. Glu-VCC combines the advantages of both.

Glu-VCC reprogram tumor-associated macrophages *in vivo*

We performed *in vivo* experiments to further verify the above findings. The immunohistochemical staining results of the tumor tissue lesions are shown in Fig. 4a. The cell numbers of IL-10^{hi} and CD206^{hi} were reduced in the VCC-treated group compared with the PBS-treated group. However, the cell num-bers of IL-12^{hi} and CD86^{hi} were not significantly changed. These results, likewise, validate that VCC can reduce the number of M2-type cells, but has no ability to induce differ-entiation of TAMs into M1-type macrophages. Compared with the Glu-treated group, the Glu-VCC-treated group was more effective in increasing the cell numbers of IL-12^{hi} and CD86^{hi} in tumors (Fig. 4a). This is due to the synergistic effect of calcium carbonate and Glu. Calcium carbonate first depletes H$^+$ in the
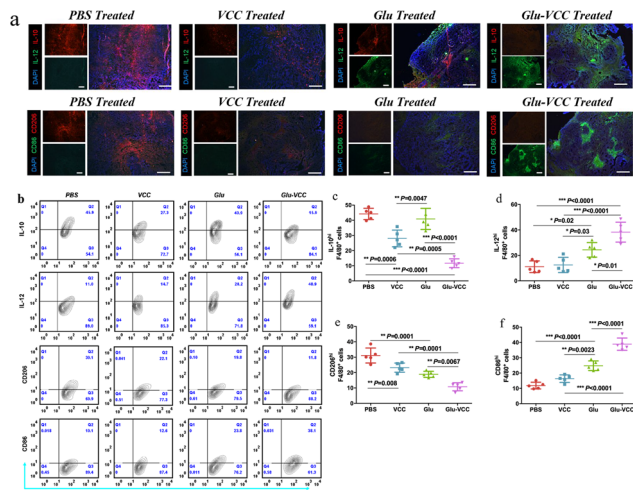
Fig. 4 Glu-VCC reprogram for the LA-induced macrophage phenotype *in vivo*. (a) The immunohistochemical staining of frozen sections of 4T1 tumor-bearing Balb/c mice; blue = nuclei, red = IL-10 or CD206, green = IL-12 or CD86 and scale = 100 μm (b) flow cytometry assays showed that IL-10^{hi}, IL-12^{hi}, CD206^{hi} and CD86^{hi} cells in the F4/80+ macrophages of tumors; (c) IL-10^{hi} F4/80+ cells; (d) IL-12^{hi} F4/80+ cells; (e) CD206^{hi} F4/80+ cells; (f) CD86^{hi} F4/80+ cells. Data for figures (c)–(f) are from figure (b) and are expressed as mean ± SD, error bars correspond to the standard deviation (n = 5) and * represents $p < 0.05$, ** stands for $0.0001 < p < 0.05$, *** stands for $p < 0.0001$.

tumor microenvironment, lifting the acidic environmental barrier and more fully exerting the effect of Glu to promote the conversion of macrophages from M2 to M1-like cells and the production of IL-12, and attenuates the secretion of IL-10.

Flow cytometry was used to further confirm the effect of Glu-VCC on the reprogramming of the macrophage phenotype. TAMs were isolated from 4T1 tumor-bearing Balb/c mouse tumors, and IL-10^{hi}, IL-12^{hi}, CD206^{hi}, and CD86^{hi} macrophages (F4/80+) were detected (shown in Fig. 4b). Compared with the PBS group, Glu did not reduce the amount of IL-10^{hi}. This was consistent with the *in vitro* results. The number of IL-10^{hi} cells decreased to 28.00% after the VCC nanoparticle treatment, suggesting that the elimination of H$^+$ from the tumor area could inhibit IL-10 expression (Fig. 4c). However, VCC nanoparticles had little effect on IL-12 expression in TAMs compared to the PBS group, indicating that VCC could not directly induce differentiation of TAMs to M1 type (Fig. 4d). This is also consistent with the results of the *in vitro* experiments. In the Glu-VCC treatment group, the percentage of IL-10^{hi} TAMs in total TAMs decreased dramatically to 11.66%, while IL12^{hi} TAMs increased to 39.12%. Meanwhile, M1-like TAMs (CD86^{hi}) reached 38.90%, while M2-like TAMs (CD206^{hi}) decreased to 10.78% (Fig. 4c–f), and the ratio of M1/M2 (M1-like TAMs divided by M2-like TAMs) was approximately 3.6 : 1. However, these data in the Glu group were approximately 1.3 : 1, and in the PBS group, M1/M2 even reached 1 : 2.6. These results suggest that drug-free Glu-VCC nanoparticles are an excellent H$^+$ scavenger and can also promote the conversion of the macrophages from M2 to M1-like cells in the tumor microenvironment through cascade effects.
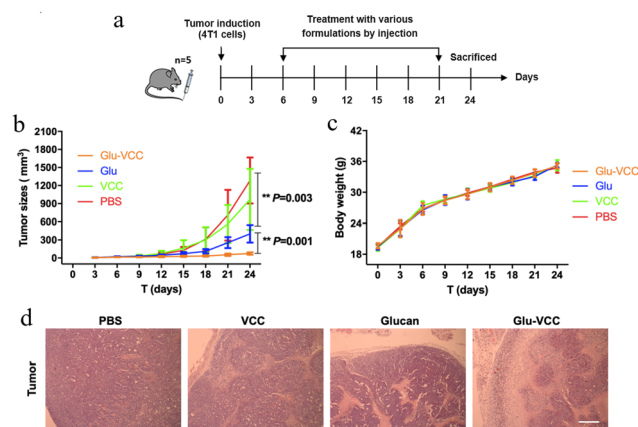

Fig. 5 Glu-VCC enhances the antitumor effect of Glu in 4T1 bearing Balb/c mice: (a) treatment schedule; (b) tumor volume changes (n = 5); (c) body weight changes (n = 5) and (d) H&E staining of tumor tissue, scale bar: 100 μm. * $p < 0.05$, ** $p < 0.01$ and *** $p < 0.001$.

Enhanced antitumor effect of Glu-VCC *in vivo*

Next, we performed *in vivo* antitumor experiments using the 4T1 tumor-bearing Balb/c mouse model to evaluate the antitumor effect of the Glu-VCC, drug-free nanoparticles. Mice were treated with different formulations (PBS, Glu, VCC, and Glu-VCC, with the same concentration of Glu and VCC). The timeline of the animal experiments is shown in Fig. 5a. The results in Fig. 5b showed that VCC had little effect on the progress of the tumor and slower tumor growth in the Glu-treated group was achieved compared to that in the PBS-treated group, which demonstrated the antitumor effect of Glu. In addition, the tumor inhibition rate in the Glu-VCC group was about 25% higher than that in the Glu group, indicating that Glu-VCC enhanced the antitumor effect of Glu. There was no significant difference in weight changes among the treatment groups (Fig. 5c). The representative H&E stained images of the tumors in Fig. 5d showed the necrotic area from each treatment. These supported that the conversion of TAMs from M2 to M1 inhibited tumor development. Glu-VCC nanoparticles improved Glu's ability to inhibit tumors. The H&E staining of the heart, liver, spleen, kidney, and lung are shown in Fig. S5 (ESI†). There were no significant differences in the morphology and structure among the groups, demonstrating the good biosafety of Glu-VCC nanoparticles.

Conclusions

We are reporting a simple co-precipitation method for the preparation of Glu-VCC. Calcium carbonate relieves the inhibition of the β-glucan immune improvement function by neutralizing H$^+$ in the tumor microenvironment, which is a unique finding of this work. In the *In vitro* experiments, the designed Glu-VCC nanoparticles effectively depleted H$^+$ from the tumor microenvironment and maintained the pH at 7.0, which promoted the conversion of TME to M1-like macrophages in the immunosuppressive microenvironment. In mice, Glu-VCC
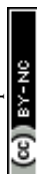
nanoparticles similarly improved the pH of the tumor region and inhibited IL-10 secretion at the tumor site, while increasing the number of the M1-like macrophages. The Glu-VCC nanoparticle-treated group reversed the M1-like/M2-like macrophage ratio from 1.3 : 1 (Glu-treated group) to approximately 3.6 : 1, greatly increasing the Glu antitumor effect. By including the remodeling of the intrinsic weak acidic and immunosuppressive microenvironment of tumors for cancer treatment, this approach may avoid the severe side effects of conventional chemotherapy and radiotherapy.[47] Glu-VCC was formulated with glucan and calcium carbonate. It offers several advantages for translational potential, such as simple composition, economy, biocompatibility, and natural targeting mechanisms. However, for successful clinical translation, the in vivo fate of the nanoparticles, with factors such as distribution, clearance, and toxicity, needs to be comprehensively evaluated. In addition, scale-up and reproducible production of the nanoparticles must be considered and investigated. Calcium carbonate as a promising material also has other excellent functions, such as triggering calcium overload in tumor cells and reducing tumor cell-induced oxidative stress.[48–50] Glu-VCC is a promising drug model, we may later combine it with photothermal therapy and photodynamic therapy, etc.,[51,52] which will contribute to the design of tumor immunotherapies and the progress of nanoparticle therapies.

Conflicts of interest

There are no conflicts to declare.

Acknowledgements

References

1 F. Geissmann, M. G. Manz, S. Jung, M. H. Sieweke, M. Merad and K. Ley, Science, 2010, 327, 656–661.

2 T. Lawrence and G. Natoli, Nat. Rev. Immunol., 2011, 11, 750–761.

3 M. Orecchioni, Y. Ghosheh, A. B. Pramod and K. Ley, Front. Immunol., 2019, 10, 1084.

4 A. Sica and A. Mantovani, J. Clin. Invest., 2012, 122, 787–795.

5 Y.-C. Wang, F. He, F. Feng, X.-W. Liu, G.-Y. Dong, H.-Y. Qin, X.-B. Hu, M.-H. Zheng, L. Liang, L. Feng, Y.-M. Liang and H. Han, Cancer Res., 2010, 70, 4840–4849.

6 N. N. Parayath, A. Parikh and M. M. Amiji, Nano Lett., 2018, 18, 3571–3579.

7 A. Mantovani, S. K. Biswas, M. R. Galdiero, A. Sica and M. Locati, J. Pathol., 2013, 229, 176–185.

8 F. Ginhoux, J. L. Schultze, P. J. Murray, J. Ochando and S. K. Biswas, Nat. Immunol., 2016, 17, 34–40.

9 S. Yang, Y. Zhang, S. Lu, L. Yang, S. Yu and H. Yang, ACS Appl. Bio Mater., 2021, 4, 3214–3223.

10 A. Kulkarni, V. Chandrasekar, S. K. Natarajan, A. Ramesh, P. Pandey, J. Nirgud, H. Bhatnagar, D. Ashok, A. K. Ajay and S. Sengupta, Nat. Biomed. Eng., 2018, 2, 589–599.

11 Q. Chen, C. Wang, X. Zhang, G. Chen, Q. Hu, H. Li, J. Wang, D. Wen, Y. Zhang, Y. Lu, G. Yang, C. Jiang, J. Wang, G. Dotti and Z. Gu, Nat. Nanotechnol., 2019, 14, 89–97.

12 M. Wen, J. Ouyang, C. Wei, H. Li, W. Chen and Y.-N. Liu, Angew. Chem., Int. Ed., 2019, 58, 17425–17432.

13 M. S. Goldberg, Nat. Rev. Cancer, 2019, 19, 587–602.

14 Y. Zhang, L. Wu, Z. Li, W. Zhang, F. Luo, Y. Chu and G. Chen, Biomacromolecules, 2018, 19, 2098–2108.

15 M. O. Li, Y. Y. Wan, S. Sanjabi, A.-K. L. Robertson and R. A. Flavell, Annu. Rev. Immunol., 2006, 24, 99–146.

16 D. M. Mosser and J. P. Edwards, Nat. Rev. Immunol., 2008, 8, 958–969.

17 G. C.-F. Chan, W. K. Chan and D. M.-Y. Sze, J. Hematol. Oncol., 2009, 2, 25.

18 M. Liu, F. Luo, C. Ding, S. Albeituni, X. Hu, Y. Ma, Y. Cai, L. McNally, M. A. Sanders, D. Jain, G. Kloecker, M. Bousamra, II, H.-G. Zhang, R. M. Higashi, A. N. Lane, T. W. M. Fan and J. Yan, J. Immunol., 2015, 195, 5055–5065.

19 P. de Graaff, C. Berrevoets, C. Rösch, H. A. Schols, K. Verhoef, H. J. Wichers, R. Debets and C. Govers, Cancer Immunol. Immunother., 2021, 70, 547–561.

20 S. C. Stone, R. A. M. Rossetti, K. L. F. Alvarez, J. P. Carvalho, P. F. R. Margarido, E. C. Baracat, M. Tacla, E. Boccardo, K. Yokochi, N. P. Lorenzi and A. P. Lepique, J. Leukocyte Biol., 2019, 105, 1041–1054.

21 O. R. Mahon, D. C. Browe, T. Gonzalez-Fernandez, P. Pitacco, I. T. Whelan, S. Von Euw, C. Hobbs, V. Nicolosi, K. T. Cunningham, K. H. G. Mills, D. J. Kelly and A. Dunne, Biomaterials, 2020, 239, 119833.

22 X. Jing, H. Hu, Y. Sun, B. Yu, H. Cong and Y. Shen, Small Methods, 2022, 6, 2101437.

23 C. Corbet, E. Bastien, N. Draoui, B. Doix, L. Mignion, B. F. Jordan, A. Marchand, J.-C. Vanherck, P. Chaltin, O. Schakman, H. M. Becker, O. Riant and O. Feron, Nat. Commun., 2018, 9, 1208.

24 M. Peng, D. Yang, Y. Hou, S. Liu, M. Zhao, Y. Qin, R. Chen, Y. Teng and M. Liu, Cell Death Dis., 2019, 10, 228.

25 J. A. Mosier, S. C. Schwager, D. A. Boyajian and C. A. Reinhart-King, Clin. Exp. Metastasis, 2021, 38, 343–359.

26 M. G. Vander Heiden, L. C. Cantley and C. B. Thompson, Science, 2009, 324, 1029–1033.

27 M. Certo, C.-H. Tsai, V. Pucino, P.-C. Ho and C. Mauro, Nat. Rev. Immunol., 2021, 21, 151–161.

28 J. X. Wang, S. Y. C. Choi, X. Niu, N. Kang, H. Xue, J. Killam and Y. Wang, Int. J. Mol. Sci., 2020, 21, 8363.

29 O. R. Colegio, N.-Q. Chu, A. L. Szabo, T. Chu, A. M. Rhebergen, V. Jairam, N. Cyrus, C. E. Brokowski, S. C. Eisenbarth, G. M. Phillips, G. W. Cline, A. J. Phillips and R. Medzhitov, Nature, 2014, 513, 559–563.

30 T. Bohn, S. Rapp, N. Luther, M. Klein, T.-J. Bruehl, N. Kojima, P. Aranda Lopez, J. Hahlbrock, S. Muth, S. Endo, S. Pektor, A. Brand, K. Renner, V. Popp, K. Gerlach, D. Vogel, C. Lueckel, D. Arnold-Schild, J. Pouyssegur, M. Kreutz, M. Huber, J. Koenig, B. Weigmann, H.-C. Probst, E. von

Stebut, C. Becker, H. Schild, E. Schmitt and T. Bopp, *Nat. Immunol.*, 2018, **19**, 1319–1329.

31 X. Chen, A. Jaiswal, Z. Costliow, P. Herbst, E. A. Creasey, N. Oshiro-Rapley, M. J. Daly, K. L. Carey, D. B. Graham and R. J. Xavier, *Nat. Immunol.*, 2022, **23**, 1063–1075.

32 F. Gao, Y. Tang, W.-L. Liu, M.-Z. Zou, C. Huang, C.-J. Liu and X.-Z. Zhang, *Adv. Mater.*, 2019, **31**, 1904639.

33 H. Wang, C. Wu, X. Tong and S. Chen, *J. Controlled Release*, 2023, **353**, 727–737.

34 K. Li, C. Lin, Y. He, L. Lu, K. Xu, B. Tao, Z. Xia, R. Zeng, Y. Mao, Z. Luo and K. Cai, *ACS Nano*, 2020, **14**, 14164–14180.

35 M. Chao, H. Wu, K. Jin, B. Li, J. Wu, G. Zhang, G. Yang and X. Hu, *eLife*, 2016, **5**, e15691.

36 H. Li, X. Zhang, X. Lin, S. Zhuang, Y. Wu, Z. Liu, J. Rong and J. Zhao, *J. Mater. Chem. B*, 2020, **8**, 1223–1234.

37 X.-Y. He, X.-H. Ren, Y. Peng, J.-P. Zhang, S.-L. Ai, B.-Y. Liu, C. Xu and S.-X. Cheng, *Adv. Mater.*, 2020, **32**, 2000208.

38 D. B. Trushina, T. N. Borodina, S. Belyakov and M. N. Antipina, *Mater. Today Adv.*, 2022, **14**, 100214.

39 Z. Dong, L. Feng, Y. Hao, M. Chen, M. Gao, Y. Chao, H. Zhao, W. Zhu, J. Liu, C. Liang, Q. Zhang and Z. Liu, *J. Am. Chem. Soc.*, 2018, **140**, 2165–2178.

40 X. Wan, H. Zhong, W. Pan, Y. Li, Y. Chen, N. Li and B. Tang, *Angew. Chem., Int. Ed.*, 2019, **58**, 14134–14139.

41 A. Som, R. Raliya, K. Paranandi, R. A. High, N. Reed, S. C. Beeman, M. Brandenburg, G. Sudlow, J. L. Prior, W. Akers, A. Y. Mah-Som, L. Habimana-Griffin, J. Garbow, J. E. Ippolito, M. D. Pagel, P. Biswas and S. Achilefu, *Nanomedicine*, 2018, **14**, 169–182.

42 A. Som, R. Raliya, L. Tian, W. Akers, J. E. Ippolito, S. Singamaneni, P. Biswas and S. Achilefu, *Nanoscale*, 2016, **8**, 12639–12647.

43 J. Liu, Q. Chen, L. Feng and Z. Liu, *Nano Today*, 2018, **21**, 55–73.

44 C. Wang, C. Ma, L. Gong, Y. Guo, K. Fu, Y. Zhang, H. Zhou and Y. Li, *Front. Immunol.*, 2021, **12**, 5381.

45 H.-c Zhou, Y. Xin-yan, W.-w Yu, X.-q Liang, X.-y Du, Z.-c Liu, J.-p Long, G.-h Zhao and H.-b Liu, *Int. Rev. Immunol.*, 2022, **41**, 4–18.

46 S. Ishihara, K. Hata, K. Hirose, T. Okui, S. Toyosawa, N. Uzawa, R. Nishimura and T. Yoneda, *Sci. Rep.*, 2022, **12**, 6261.

47 X. Zhu, N. Xu, L. Zhang, D. Wang and P. Zhang, *Eur. J. Med. Chem.*, 2022, **238**, 114456.

48 Y. Li, S. Zhou, H. Song, T. Yu, X. Zheng and Q. Chu, *Biomaterials*, 2021, **277**, 121080.

49 C. Wang, F. Yu, X. Liu, S. Chen, R. Wu, R. Zhao, F. Hu and H. Yuan, *Adv. Healthcare Mater.*, 2019, **8**, 1900501.

50 Y. Wu, W. Gu, J. Tang and Z. P. Xu, *J. Mater. Chem. B*, 2017, **5**, 7194–7203.

51 W. Zhong, K. H. Wong, F. Xu, N. Zhao and M. Chen, *Acta Biomater.*, 2022, **145**, 135–145.

52 P. Xue, M. Hou, L. Sun, Q. Li, L. Zhang, Z. Xu and Y. Kang, *Acta Biomater.*, 2018, **81**, 242–255.